

ELECTRONIC SUPPLEMENTARY INFORMATION

Novel Adamantane-based Hole Transport Materials for Perovskite Solar Cells: A
Computational Approach

Maebienne Anjelica B. Gapol and Dong Hee Kim*

Department of Chemistry, Kunsan National University, Kunsan, 573-701, Republic of Korea

Table S1. Difference of the calculated adiabatic ground state oxidation potential (GSOP_a) from the experimental HOMO ($\text{HOMO}_{\text{expt}}$) of Ad-OMeTPA calculated at DFT/6-31G(d,p) in DCM.

Exchange-Correlation Density Functionals		
Global Hybrid	Difference (GSOP_a - $\text{HOMO}_{\text{expt}}$) (eV)	
B3LYP	0.23	
APF	0.13	
SOGGA11X	-0.05	
BHandHLYP	-0.21	
Range-Separated Hybrid	ω (Bohr ⁻¹)	Difference (eV)
LC- ω PBE	0.40	-1.01
CAM-B3LYP	0.33	-0.36
	0.20	-0.13
	0.175	-0.07
	0.15	0.00

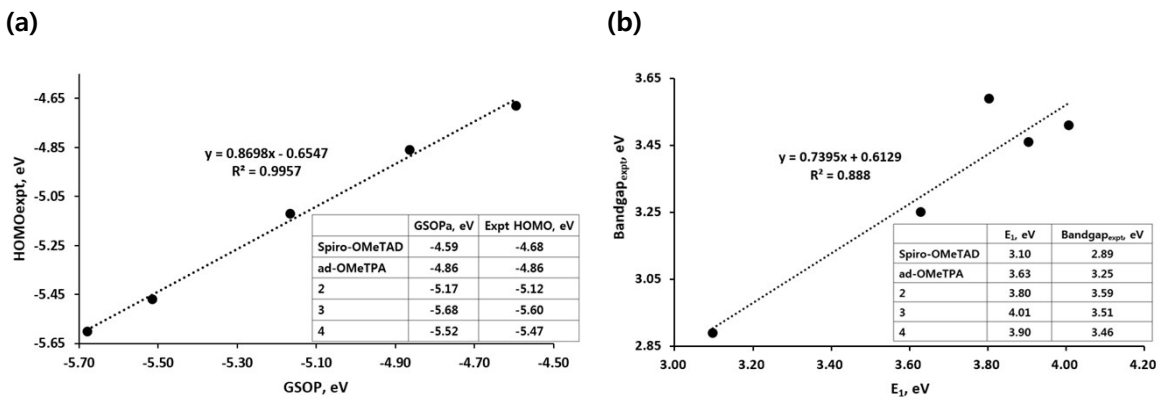


Figure S1. (a) Linear correlation of the experimental HOMO ($\text{HOMO}_{\text{expt}}$) versus the calculated ground state oxidation potential (GSOP) of the reference molecules^{1, 2} calculated using CAM-B3LYP/6-31G(d,p), $\omega=0.15$ in DCM. (b) Linear correlation of the experimental bandgap ($\text{Bandgap}_{\text{expt}}$) and first excited state energy (E_1) calculated using TD-DFT//CAM-B3LYP/6-31G(d,p) in DCM.

Table S2. Difference of the calculated first excited state energy (E_1) and experimental optical band gap ($E_{g,\text{expt}}$) using TD-DFT//CAM-B3LYP/6-31G(d,p) in DCM.

Exchange-Correlation Density Functionals	Difference ($E_1 - E_{g,\text{expt}}$) (eV)
B3LYP/6-31G(d,p)	0.38
SOGGA11-X/6-31G(d,p)	0.88
CAM-B3LYP/6-31G(d,p)	0.97

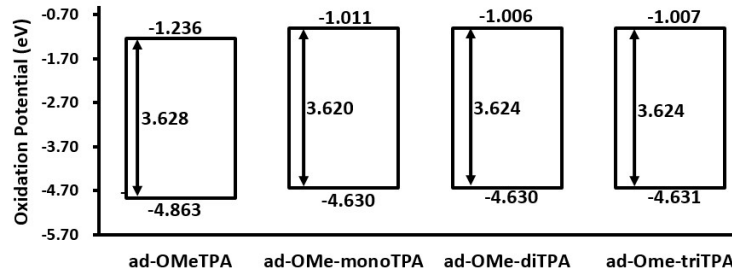


Figure S2. Ground state oxidation potential (GSOP) and excited state oxidation potential (ESOP) of the adamantane derivatives calculated using CAM-B3LYP with $\omega=0.15$ and TD-B3LYP//CAM-B3LYP, respectively, in DCM.

Table S3. Hole reorganization energy (λ_h) and its components (λ^+ and λ^0) calculated at CAM-B3LYP with $\omega=0.15$ in DCM.

	λ_h (eV)	λ^+ (eV)	λ^0 (eV)
ad-OMeTPA	0.125	0.067	0.058
ad-OMe-monoTPA	0.232	0.120	0.112
ad-OMe-diTPA	0.237	0.124	0.113
ad-Ome-triTPA	0.444	0.330	0.114
Spiro-OMeTAD	0.139	0.067	0.073
ad-EtTPA	0.048	0.022	0.025
ad-tBuTPA	0.316	0.248	0.068
ad-SMeTPA	0.343	0.265	0.078
ad-NMeTPA	0.571	0.408	0.163

Table S4. The calculated dihedral angles of the optimized neutral and cationic geometries of the adamantane derivatives at CAM-B3LYP with $\omega=0.15$ in DCM.

		ad-OMeTPA			ad-EtTPA			ad-tBuTPA		
Quad rant	Desig nation	Neutral	Cation	$ \Delta\phi $	Neutral	Cation	$ \Delta\phi $	Neutral	Cation	$ \Delta\phi $
Q1	D1	32.100	31.172	0.927	38.813	35.702	3.111	38.608	37.555	1.053
	D2	30.915	30.530	0.385	38.847	36.357	2.490	39.979	39.103	0.876
	D3	0.143	0.131	0.012	-87.514	-88.474	0.960	-58.922	-59.053	0.130
	D4	0.475	0.299	0.176	-88.638	-87.100	1.538	-0.622	-0.609	0.013
Q2	D1	32.159	35.402	3.243	37.811	34.814	2.997	37.391	36.099	1.292
	D2	33.621	35.510	1.889	37.991	34.797	3.194	36.378	35.303	1.075
	D3	0.460	-0.158	0.618	-89.966	-88.606	1.360	-59.763	-60.048	0.285
	D4	0.506	-0.148	0.654	-86.576	-87.480	0.904	-59.893	-60.039	0.146
Q3	D1	30.915	30.531	0.384	38.834	35.700	3.134	39.457	35.604	3.853
	D2	32.100	31.172	0.928	38.800	35.109	3.691	39.235	35.164	4.071
	D3	0.475	0.299	0.176	-88.649	-87.523	1.126	0.311	0.077	0.233
	D4	0.143	0.131	0.013	-87.516	-87.749	0.232	-60.087	-59.822	0.264
Q4	D1	32.159	35.409	3.250	37.818	35.990	1.828	40.030	37.750	2.280
	D2	33.621	35.518	1.897	37.999	36.760	1.239	39.712	37.782	1.931
	D3	0.460	-0.158	0.618	-89.969	-87.698	2.271	-60.041	-59.507	0.534
	D4	0.505	-0.148	0.653	-86.574	-89.034	2.460	-60.090	-59.330	0.760
		ad-SMeTPA			ad-NMeTPA					
		Neutral	Cation	$ \Delta\phi $	Neutral	Cation	$ \Delta\phi $			
Q1	D1	47.331	44.307	3.024	29.144	26.803	2.341			
	D2	46.800	44.989	1.811	29.759	26.313	3.446			
	D3	-71.560	-66.890	4.670	-13.088	-13.167	0.079			
	D4	-70.624	-72.053	1.429	-13.225	-13.289	0.063			
Q2	D1	46.697	44.605	2.093	27.600	27.389	0.211			
	D2	47.124	44.976	2.148	27.676	28.729	1.053			
	D3	-73.120	-63.068	10.051	-12.896	-12.654	0.242			
	D4	-72.375	-71.554	0.822	-13.222	-12.799	0.422			
Q3	D1	42.998	40.230	2.768	29.759	44.462	14.704			
	D2	43.732	41.575	2.158	29.145	44.498	15.353			
	D3	-1.136	-1.299	0.163	-13.224	-1.185	12.039			
	D4	-82.685	-78.294	4.391	-13.088	-1.310	11.778			
Q4	D1	42.960	42.003	0.957	27.600	27.301	0.299			
	D2	44.754	41.789	2.965	27.676	28.105	0.429			
	D3	-1.513	-1.225	0.288	-12.897	-13.110	0.213			
	D4	-77.387	-0.943	76.444	-13.221	-12.781	0.441			

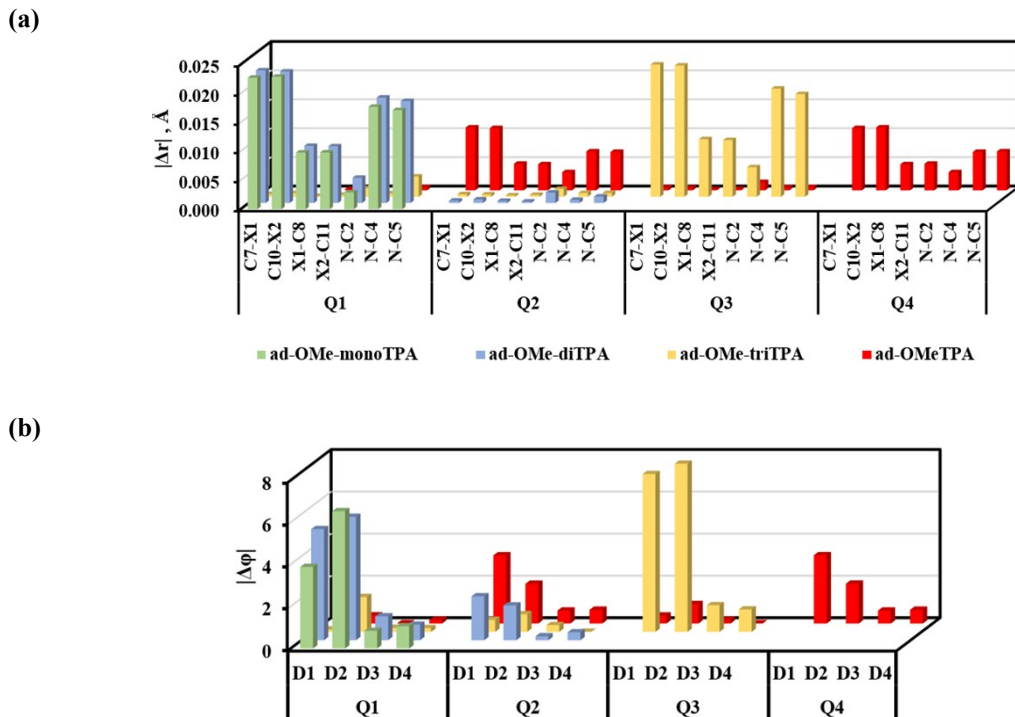


Figure S3. (a) Bond length difference (\AA) and (b) dihedral angle difference ($^{\circ}$) of the ground state neutral molecule and corresponding cationic structures of each adamantane derivatives calculated at CAM-B3LYP with $\omega=0.15$ in DCM.

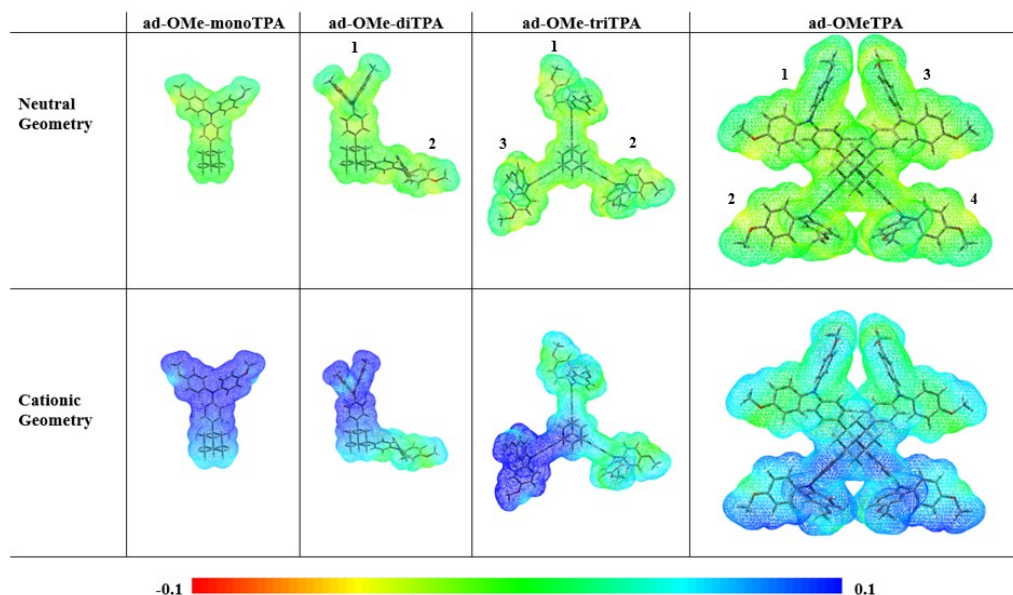


Figure S4. The ESP mapped onto the total electron density of the neutral and cationic geometries of the derivatives. Regions of high and low potentials are indicated in red and blue, respectively.

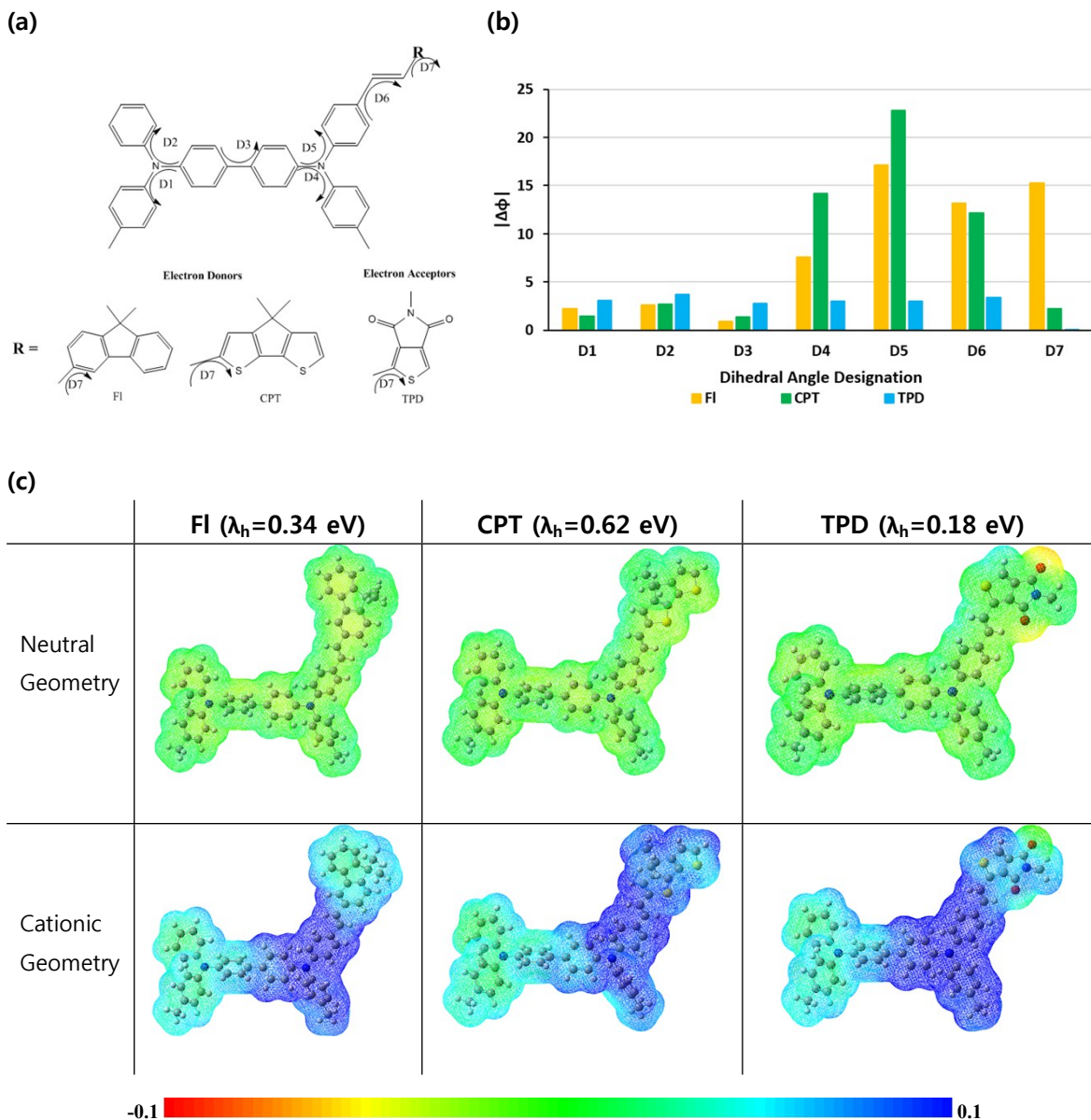


Figure S5. **(a)** Dihedral angle designation and **(b)** the absolute dihedral angle changes ($|\Delta\Phi|$) between the neutral and cationic form of TPB based molecules. **(c)** The electrostatic potential maps of the derivatives. These structures were calculated at LC- ω PBE/6-31G(d,p) in DCM.

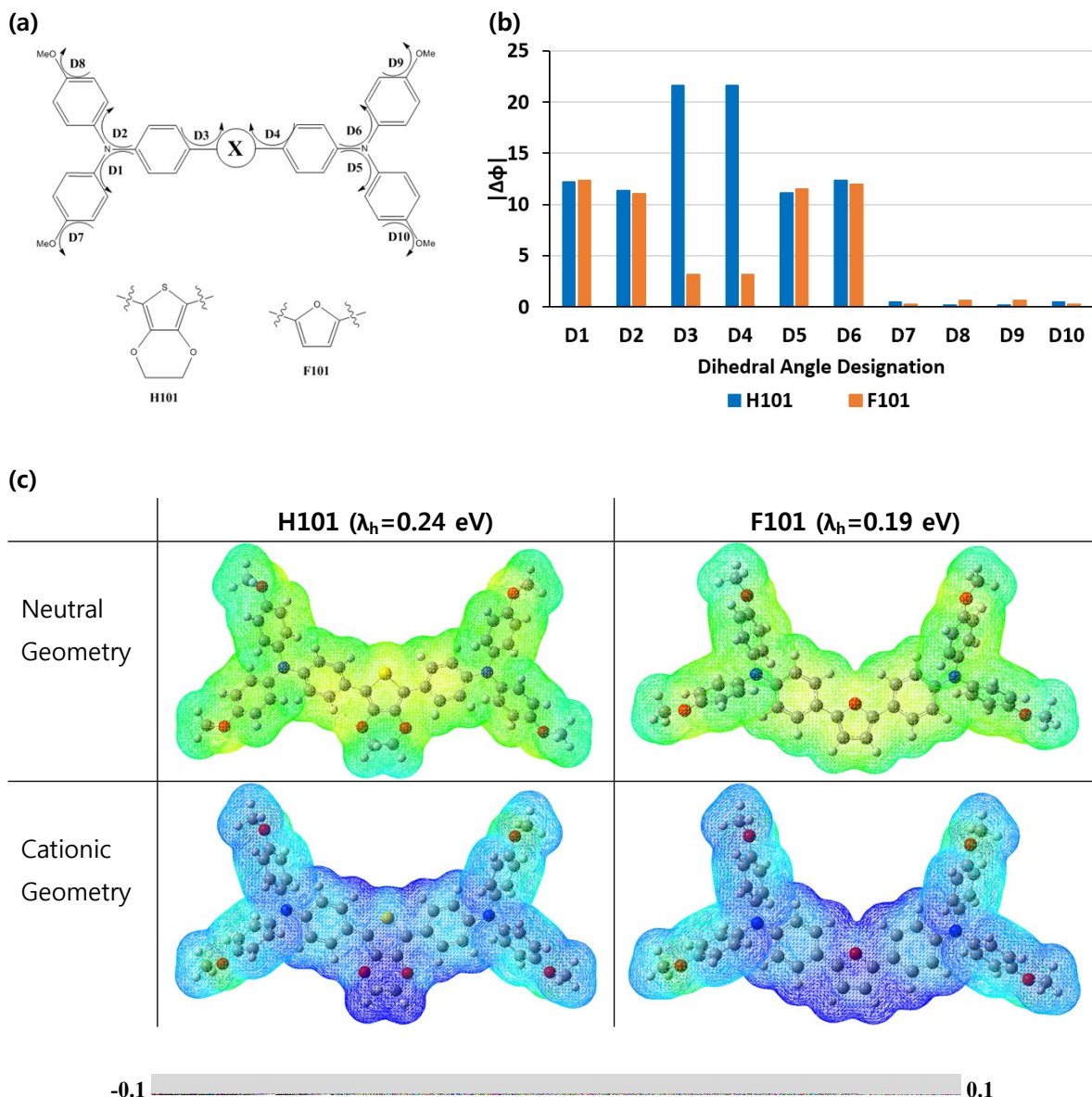


Figure S6. (a) Dihedral angle designation and (b) the absolute dihedral angle changes ($|\Delta\Phi|$) between the neutral and cationic form of TPA based molecules. (c) The electrostatic potential maps of the derivatives. These structures were calculated at LC- ω PBE/6-31G(d,p) in DCM.

References

1. Zhang, K.; Wang, L.; Liang, Y.; Yang, S.; Liang, J.; Cheng, F.; Chen, J. *Synthetic Metals* **2012**, 162, (5-6), 490-496.
2. Gu, Y.; Zhou, X.; Li, Y.; Wu, K.; Wang, F.; Huang, M.; Guo, F.; Wang, Y.; Gong, S.; Ma, D.; Yang, C. *Organic Electronics* **2015**, 25, 193-199.